ORAL/POSTER REFERENCE: ICF100540OR

INDENTATION-INDUCED DAMAGE OF THIN-FILMS SUPPORTED ON SUBSTRATES

A.H.W. Ngan and H.P. Ng

**Department of Mechanical Engineering, The University of Hong Kong,
Pokfulam Road, Hong Kong, P.R. China**

ABSTRACT

When indentation is made on a thin film supported on a substrate, the ways by which the indenter's volume can be accommodated are considered here. Depending on the relative strengths of the film and substrate, three regimes are proposed as follows: i) when the film is a lot harder than the substrate, the deformation may be modelled by assuming that the film is rigid; ii) when the film has similar strength as the substrate, the deformation pattern is likely to be spherical as similar to indentation on a homogeneous material; iii) when the film is a lot softer than the substrate, the substrate can be assumed to be rigid. Mechanistic models are proposed for the scenarios ii) and iii).

Keywords Hardness, Coatings, Sputtering, Metal Films

INTRODUCTION

Indentation on thin films supported by substrates has been an important research subject as it is often necessary to know the mechanical properties of, for example, hard protective coatings. When the indentation depth is small, say within 10% of the film thickness, the substrate effect is negligible and hence the measured hardness becomes a sole property of the film material. However, at such small values of indentation depth, the measured hardness is prone to a strong intrinsic size effect (ISE), which we term the *intrinsic* effect here as it refers to the film material alone. When the indentation depth is a significant fraction of the film thickness, the substrate effect becomes significant. To illustrate this, we use data from our recent experiments on deposited metallic alloy films [1-3]. Illustrated in Figure 1(a) are the microhardness values versus indentation depth (h) for three film thickness values (t) obtained from 3Ni/Al alloy films on pure Ni substrates. The h/t ratio is larger than 10% for all the data shown. It can be seen that the measured hardness exhibited a strong negative ISE, and the hardness results for different thickness values fall on distinct curves when plotted against h. However, when plotted against h/t in Figure 1(b), the results fall on a single curve. This indicates that, in this thickness range at least, the ISE obeys geometrical similarity with the film thickness being the characteristic length scale. To distinguish this regime from the intrinsic effect discussed above, we term this the *extrinsic* ISE. When the film remains adhered to the substrate during indentation, one may expect that the extrinsic ISE would be self-similar so that the hardness depends on h/t but not on h alone. This is the situation observed in Figure 1 (b). When film delamination occurs, the interfacial crack length represents another length scale in the problem, and so the indentation may no longer be self-similar.

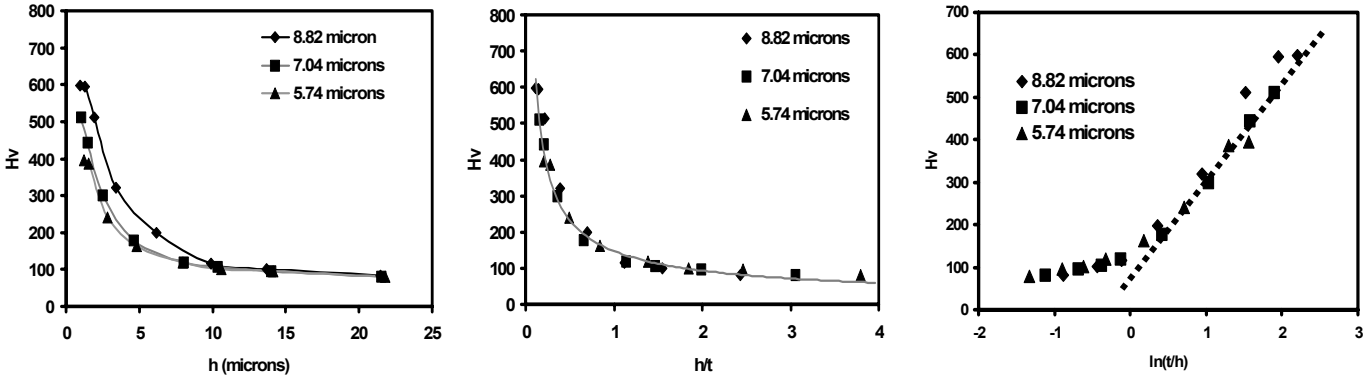

Figure 1: Vickers hardness values against (a) indentation depth h, (b) indentation depth h normalised by film thickness t, (c) ln(t/h) for 3Ni/Al films of three different thickness on pure Ni substrates [2].

If the aim of the experiment is to measure the strength of the film, the strong ISE observed, no matter intrinsic or extrinsic, would certainly make life very difficult as it would not be obvious as to which hardness value on the curve to take, and the measured hardness is no longer roughly three times the yield strength. A reliable model of the ISE would therefore be highly desirable. Since in general the intrinsic effect dominates over quite a narrow range of small indentation depth ratio, we believe it is more useful to make use of the extrinsic ISE to get information about the film strength. It is therefore the aim of this paper to bring some insight into the extrinsic ISE by proposing mechanistic models for this type of ISE.

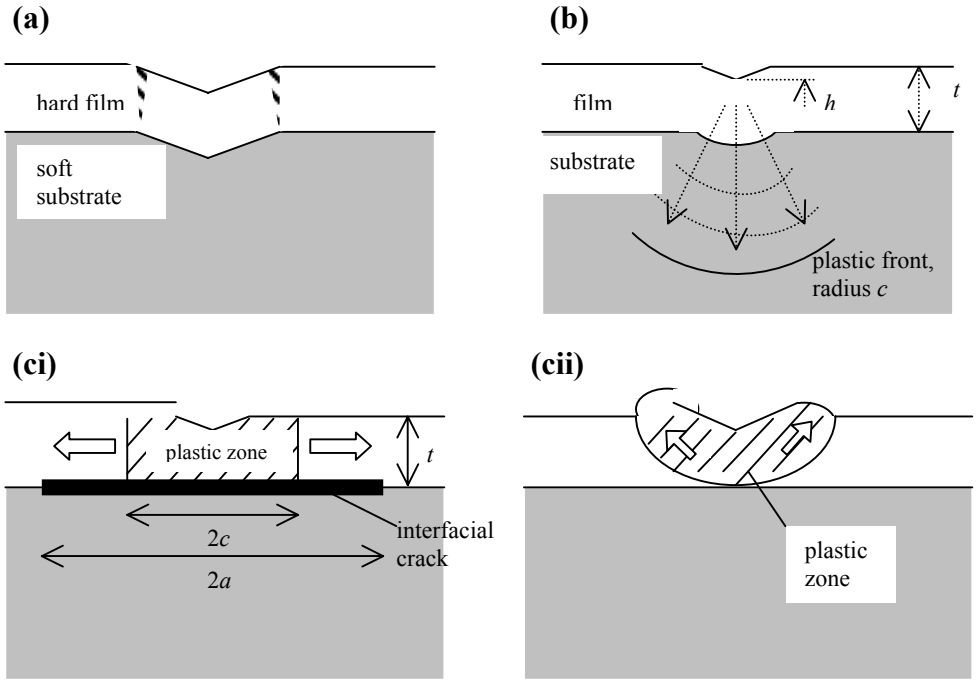

Figure 2: (a) Rigid film mode, (b) radial mode, and (ci,cii) planar modes of plastic deformation accompanying indentation on a thin film supported by substrate.

MECHANISTIC MODELS FOR EXTRINSIC ISE

In a general case of modelling indentation on a film supported by a substrate, it is useful to think of a spectrum of possibilities as shown in Figure 2. One extreme is the *rigid film mode* (Figure 2(a)) in which the film is much harder than the substrate. In this situation, the film will merely deform or crack at the hinges of the indent, and between the indent and the substrate, the film remains rigid. The scenario is therefore similar to that considered by Jönsson and Hogmark [4]. When the film has similar strength as the substrate, the film will deform together with the substrate as shown in Figure 2(b). There is little

tendency of sliding across the film/substrate interface, and depending on the strength of the interface, the film may or may not delaminate, but this should not influence the material flow to a significant extent. We denote this mode as the *radial mode*. The other extreme is to have a very soft film on a hard substrate as shown in Figure 2(c). In this situation, the film material under the indent will be squashed by the indenter, but the substrate will have little deformation. A large shear stress will be set up across the film/substrate interface. If the interface is weak, it will then crack. Once film delamination has occurred, the indentation volume is accommodated mainly by pushing the film material surrounding the indentation core in a more or less co-planar fashion along the film as shown in Figure 2(ci). There will be relative sliding of the film material over the substrate, and when the delamination crack size is large enough, the elastic portion of the delaminated film may buckle upward. This mode is in fact similar to that considered by Evans and Hutchinson [5] who have also provided experimental evidence for its existence. We denote this here as the *planar mode*. If the interface is strong so that the film does not delaminate, the film material is difficult to flow radially outward in a co-planar fashion, so that the only way to accommodate the indenter volume would be to flow upward to as shown in Figure 2(cii). We term this the *pile-up* mode. Since the ISE of the rigid film mode in Figure 2(a) has already been considered by Jönsson and Hogmark [4], and the pile-up mode is difficult to model analytically, we will focus on the remaining two modes in the rest of this paper.

RADIAL MODE

When the film has similar strength as the substrate, the material flow pattern should not differ significantly from that in the indentation on a homogeneous half space. The latter has been modelled rather successfully using the cavity model [6]. For a convenient analytical model for the radial mode in thin-film, we will therefore follow the assumptions of this model. Hence, as a crude approximation, we assume in Figure 2(b) that the mean pressure p_o underneath the indenter creates plastic flow of material residing mainly inside a spherical plastic zone which is a sector of a hemisphere subtended at the centre of the indent. This is more likely the case for blunt indenters like Vickers or Berkovich. Let c be the radius of this plastic zone, and r the radial distance of a point inside this plastic zone. Assuming spherical field inside the plastic zone, equilibrium requires $\partial\sigma_r / \partial r = 2(\sigma_\theta - \sigma_r)/r$, where σ_r and σ_θ are the radial and hoop stresses respectively. With the Tresca criterion σ_θ - $\sigma_r = Y_i$, where Y is yield stress and the subscript i denotes either the film (f) or the substrate (s), the stress solutions are:

$$\sigma_r = \begin{cases} -2Y_f \ln\left(\frac{t}{r}\right) - 2Y_s \ln\left(\frac{c}{t}\right) - \frac{2Y_s}{3} & \text{for } r \le t \text{ (the film)} \\ -2Y_s \ln\left(\frac{c}{r}\right) - \frac{2Y_s}{3} & \text{for } c > r \ge t \text{ (the substrate).} \end{cases} \quad (1)$$

In deriving eqn. (2), the integration constants are chosen such that the radial stresses are matched across the film/substrate interface, and the boundary between the plastic zone and the elastic outer region for $r > c$ which is also assumed to be spherical. The mean pressure inside the indent core $r < h \tan\Psi$, where h is the depth of the indent and Ψ the semi-angle of the indenter, is given by:

$$p_o = -\sigma_r\big|_{r=h\tan\Psi} = 2Y_f \ln\left(\frac{t}{h\tan\Psi}\right) + 2Y_s \ln\left(\frac{c}{t}\right) + \frac{2Y_s}{3}. \quad (2)$$

The plastic front at $r = c$ can be located by considering compressibility inside the plastic zone in a similar fashion as was done previously [6]. Defining $v = \mathrm{d}u(r)/\mathrm{d}c$ as the rate of change of position u of a material point inside the plastic zone at r with respect to the plastic zone size c, the assumption of incompressibility leads to $\partial v / \partial r + 2v/r = 0$ for $c > r > h \tan\Psi$. Solution to this which matches the elastic region at $r = c$ is

$$\upsilon = \frac{3Y_s c^2}{2E_s r^2}, \quad c > r > h\tan\Psi, \tag{3}$$

where E_s is the Young's modulus of the substrate material. Noting that if the volume of the indent core is to be conserved during a depth increment of dh, $2\pi h^2\tan^2\Psi\,\mathrm{d}u(h\tan\Psi) = \pi h^2\tan^2\Psi\,\mathrm{d}h$. Hence, from eqn. (3),

$$\frac{c}{h} = \left(\frac{E_s\tan^2\Psi}{3Y_s}\right)^{1/3}. \tag{4}$$

Since the measured hardness $H \approx p_o$, substituting eqn. (4) into eqn. (2) gives

$$H = H_o + 2(Y_f - Y_s)\ln\left(\frac{t}{h}\right), \quad H_o = -2Y_f\ln(\tan\Psi) + \frac{2Y_s}{3}\left[\ln\left(\frac{E_s\tan^2\Psi}{3Y_s}\right) + 1\right]. \tag{5}$$

H_o is independent of t and h. Eqn. (5) indicates a falling trend of hardness versus indentation depth, i.e. a negative ISE, when $Y_f > Y_s$, and a positive ISE when $Y_f < Y_s$.

In terms of applicability, the radial mode consideration here is subject to two limits. The first is that the indent size must be large enough to make the plastic zone spread well beyond the film/substrate interface, so that the presence of the substrate can be felt. The second limit is that for the cavity model to be a good approximation, the deformation field must stay more or less spherical. This will not be the case when the film and substrate have too different yield properties, or the indent is too deep compared with the film thickness. For the latter, if the indenter penetrates deeply into the substrate, it may be expected that the film profile would conform gradually to the indenter shape even if it does not break, and so the flow field would deviate significantly from being spherical. An intuitive estimate for the field to maintain roughly spherical is that $h/t \ll 1$.

PLANAR MODE

The planar mode is similar to the situation considered by Evans and Hutchinson [5], who have assumed that the plastic and elastic zones reside entirely in the delaminated film. This is likely to be the case when the substrate is non-deformable and the film/substrate interface is weak. Here we follow a similar line of development but focus more on the interaction between the plastic zone and the elastic zone. We assume that the plastic zone surrounding the indent is a disk with radius c as shown in Figure 2(ci). Surrounding this is the elastic zone, which extends from $r = c$ to $r = a$, where a is the radius of the penny shape interfacial crack. From volume conservation of the plastic zone, Evans and Hutchinson [5] showed that the radial displacement at the plastic/elastic boundary, Δ, is given by

$$u(r = c) = \Delta = \frac{\pi h^3\tan^2\Psi}{6ct}. \tag{6}$$

Since the displacement beyond interfacial crack radius may be assumed to be negligible,

$$u(r = a) \approx 0. \tag{7}$$

The elastic stress solutions which satisfy eqns. (6) and (7) are

$$\sigma_r = \frac{cE_f\Delta}{c^2-a^2}\left[\frac{1}{(1-\nu_f)}+\frac{1}{(1+\nu_f)}\frac{a^2}{r^2}\right],\ \ \sigma_\theta = \frac{cE_f\Delta}{c^2-a^2}\left[\frac{1}{(1-\nu_f)}-\frac{1}{(1+\nu_f)}\frac{a^2}{r^2}\right],\qquad a \le r \le c, \tag{8}$$

where E_f and ν_f are respectively Young's modulus and Poisson's ratio for the film material. The elastic energy residing in the elastic region is given by

$$U = -\pi c t \Delta \sigma_r (r = c). \tag{9}$$

The elastic energy release rate $G = -1/(2\pi a)\,(\partial U/\partial a)$ and from eqns. (8) & (9),

$$G = \frac{2c^2 t E_f \Delta^2}{(a^2-c^2)^2}. \tag{10}$$

This expression for G is somewhat different from that of Evans and Hutchinson because here we consider a radial field according to eqn. (8) but in Evans and Hutchinson, a uniform compressive stress state was assumed. A stable crack size will occur when $G = K_{II}^2(1-\nu_f^2)/E_f$, where K_{II} is the mode II critical stress intensity factor of the film/substrate interface. From eqn. (10), this stable crack size is given by:

$$a^2 = c^2 + \frac{cE_f\Delta}{K_{II}}\sqrt{\frac{2t}{1-\nu_f{}^2}}. \tag{11}$$

The plastic zone radius is located by noting that at the elastic/plastic boundary at $r = c$, $\sigma_\theta - \sigma_r = Y_f$. From eqns. (6), (8) & (11), this requires

$$\frac{h^3}{c^2 t} = \frac{6(1+\nu_f)}{\pi E_f \tan^2\Psi}\left[\frac{Y_f}{2}-\frac{K_{II}}{\sqrt{t}}\sqrt{\frac{(1-\nu_f)}{2(1+\nu_f)}}\right]. \tag{12}$$

To relate the measured hardness with the plastic zone, a descriptive model must be assumed for the latter. For a blunt indenter, the region outside the indent core but inside the plastic zone, i.e. $c \le r \le h\tan\Psi$, may be assumed to be subject principally to plane stress. The equilibrium condition for this region may therefore be written as $\partial\sigma_r/\partial r = (\sigma_\theta - \sigma_r)/r = Y_f/r$. Solution of this is

$$\sigma_r = Y_f \ln\left(\frac{r}{c}\right) + \sigma_r(r=c), \quad c \le r \le h\tan\Psi. \tag{13}$$

The mean pressure p_o supporting the indenter is approximately equal to $-\sigma_r(r = h\tan\Psi)$. Thus, from eqns. (13), (10), (11) & (12),

$$p_o = \frac{Y_f}{2}\ln\left(\frac{h}{t}\right)+\frac{Y_f}{2}+\frac{K_{II}}{\sqrt{t}}\left[\sqrt{\frac{2}{1-\nu_f{}^2}}-\sqrt{\frac{(1-\nu_f)}{2(1+\nu_f)}}\right]-\frac{Y_f}{2}\ln\left[\frac{6(1+\nu_f)}{\pi E_f}\left(\frac{Y_f}{2}-\frac{K_{II}}{\sqrt{t}}\sqrt{\frac{(1-\nu_f)}{2(1+\nu_f)}}\right)\right]. \tag{14}$$

The measured hardness thus has the form

$$H = \frac{Y_f}{2}\ln\left(\frac{h}{t}\right)+H_1 \tag{15}$$

where $H_1 = Y_f f(E_f / Y_f, \nu_f, K_{II} / Y_f \sqrt{t})$ comprises the last three terms in eqn. (14) and is a term independent of *h*. Eqn. (15) indicates that for the planar mode, *H* will increase with the indentation depth, i.e. a positive ISE will result.

As discussed by Evans and Hutchinson [5], buckling of the elastic region $a \leq r \leq c$ may occur for sufficiently large p_o. They have shown using a post-buckling theory that this is equivalent to reducing K_{II} by a factor $\sqrt{\alpha}$, where α (<1) is a parameter indicating the post-buckling stiffness of the film material. With this correction when the film buckles, the form of the depth dependence of *H* in eqn. (15) is unchanged.

COMPARISON WITH EXPERIMENTS

Because of space limitation, we will only discuss the radial mode here. Experimental results involving planar model will be dealt with in a forthcoming publication. For the radial mode, we use the hardness results on 3Ni/Al alloy films on nickel substrates shown in Figure 1(a). These were sputtered films and the experimental procedures have already been described elsewhere [1-3,7]. Being metallic films, they should be deformable and hence such a material system should represent a good prototype for the radial mode. As mentioned earlier, Figure 1(b) shows that the observed ISE obeys geometrical similarity, and one may also notice from eqn. (5) that the predicted ISE for the radial model also obeys similarity. In Figure 1(c) are shown the hardness results plotted against ln(*t*/*h*). It can be seen that the variation is approximately bilinear, with the turning point occurring at $h \approx t$, i.e. at the situation where pierce-through is about to occur. The segment on the left of the turning point corresponds to the post-pierce-through situation and since the apparent hardness at increasing load should approach that of the substrate, this segment should deviate in the long run from the apparent linearity shown in Figure 1(c) when ln(*t*/*h*) becomes increasingly negative. On the right of the turning point, i.e. for the situation before pierce-through occurs, it can be seen that the data fall reasonably accurately on a common straight line in agreement with eqn. (5). The measured slope of this straight line is ~ 2.30 GPa. Hence, from eqn. (5), Y_f should be larger than Y_s by about 1.15 GPa. The hardness of the Ni substrate is 1 GPa, and hence its yield stress is about 0.33 GPa. The estimated yield stress of the 3Ni/Al film is therefore about 1.5 GPa. In ref. [3], more results on alloy thin films are compared with the prediction in eqn. (5). To summarise, by comparing an experimental hardness vs depth variation with eqn. (5), the yield strength of a thin film supported on a substrate can be obtained.

ACKNOWLEDGMENTS

This research was supported by a grant from the Research Grants Council of the Hong Kong Special Administrative Region, China (Project no. HKU 7077/00E), and a CRCG grant from the University of Hong Kong (Project no. 10202005/16180/14500/301/01).

REFERENCES

1. Ng, H.P., Meng, X.K. and Ngan, A.H.W. (1998) *Scripta Mater*. 39, 1737.
2. Ng, H.P. (2000) Ph.D. Thesis, University of Hong Kong.
3. Li, S.Y., Ng, H.P. and Ngan, A.H.W. (2001) to appear in "Fundamentals of Nanoindentation and Nanotribology," ed. S. P. Baker, R. F. Cook, S. G. Corcoran, and N. R. Moody, Mater. Res. Soc. Symp. Proc..
4. Jönsson, B. and Hogmark, S. (1984) *Thin Solid Films* 114, 257.
5. Evans, A.G. and Hutchinson, J.W. (1984) *Int. J. Solids Structures* 20, 455.
6. Johnson, K.L. (1985) *Contact Mechanics*. Cambridge University Press, p. 172.
7. Ng, H.P. and Ngan, A.H.W. (2000) *J. Appl. Phys*. 88, 2609.